OCEANS AND ATMOSPHERE
www.csiro.au

The aerial survey index of abundance: 2017 updated results

Paige Eveson and Jessica Farley
CCSBT-ESC/1708/06

Prepared for the Extended Scientific Committee for the Twenty Second Meeting of the Scientific Committee, Yogyakarta, Indonesia, 28 August -2 September, 2017

Citation

Eveson P, Farley J (2017). The aerial survey index of abundance: 2017 updated results. ESC/1708/06, Twenty Second Meeting of the Scientific Committee, Yogyakarta, Indonesia, 28 August -2 September, 2017

Acknowledgments

There are many people we would like to recognise for their help and support during this project. We would especially like to thank this year's spotter-pilot, spotter and data recorder; Felicity Brown, Wade Austin, Micah Landon-Lane, John Veerhuis. We also appreciate the support given to us by the commercial tuna spotters and pilots during the survey especially for providing information on weather condition during flights. This study was funded by CCSBT members and CSIRO Oceans and Atmosphere.

Contents

1 Abstract

The estimate of relative abundance of juveniles from the 2017 scientific aerial survey is similar to the 2014 estimate, and significantly above the long-term average. Although it is much lower than the 2016 estimate, the 2016 estimate was anomalously high. The survey was not conducted in 2015 due to funding issues, so we do not have a 2015 estimate for comparison.

The environmental conditions during the 2017 survey were average for the most part, except that wind speed tended to be lower and swell height slightly higher than usual. In terms of the models that standardize the index to average conditions, these work in opposite directions since fewer sightings would have been expected if wind speed was higher but more sightings would have been expected if swell was lower. Air temperature was also lower than average, but this variable is not used in the standardization process (rather sea surface temperature is used, which was very close to the long-term average).

Most sightings were made inshore in the eastern half of the survey area. As in the 2009-2013 surveys, a high percentage of the observed total biomass coming from schools comprised of small fish (<8 kg) was observed again this year (13.8%).

2 Introduction

The index of juvenile southern bluefin tuna (SBT) abundance based on a scientific aerial survey in the Great Australian Bight (GAB) is one of the few fishery-independent indices available for monitoring and assessment of the SBT stock. The aerial survey was conducted in the GAB between 1991 and 2000, but was suspended in 2001 due to logistic problems of finding trained, experienced observers (spotters). The suspension also allowed for further data analysis and an evaluation of the effectiveness of the survey. A decision to continue or end the scientific aerial survey could then be made on the merits of the data, in particular the ability to detect changes in abundance.

Analysis of the data was completed in 2003 and it showed that the scientific aerial survey does provide a suitable indicator of SBT abundance in the GAB (Bravington 2003). In the light of serious concerns about the reliability of historic and current catch and CPUE data and weak year classes in the late 1990s and early 2000s, this fishery-independent index was considered even more important (Anon 2008). Thus, in 2005, the full scientific line-transect aerial survey was re-established in the GAB, and this survey has been conducted each year since, except in 2015. New analysis methods were developed and have subsequently been refined. Based on these methods, an index of abundance across all survey years has been constructed.

Up until 2010, all planes that flew in the survey had two spotters – a spotting pilot and a dedicated spotter – each searching his own side of the plane. Due to the retirement of the two spotting pilots involved in recent surveys, and the inability to replace them, one of the two planes flying in the 2010 survey and both planes flying in the 2011 to 2014 surveys had only one spotter (along with a non-spotting pilot). Solo spotters need to search both sides of the plane and are likely to miss more sightings than two spotters. In anticipation of this significant change to the survey, calibration experiments were run in parallel with the full scientific aerial survey in 2007-2009 (see Eveson et al. 2007, 2008, 2009 for details). The 2007 experiment served as a pilot study that led to improvements in the design of the 2008 and 2009 experiments. These latter experiments were designed to compare the number of SBT sightings and total estimated biomass of SBT observed by a single spotter in the calibration plane versus two spotters in the survey plane over the same area and time strata. Based on data from these experiments, a method for accounting for the fact that a plane with one observer makes fewer sightings than a plane with two observers was developed in Eveson et al. (2009, 2010) and refined in Eveson et al. (2011). These methods have been applied to the analysis since 2011.

There was no scientific aerial survey in 2015 due to lack of agreement on funding arrangements. The CCSBT members agreed to fund a reduced aerial survey in 2016 that used one plane for three months. A new spotter was calibrated into the survey in 2016 (Eveson & Farley 2016). The CCSBT members agreed to fund a reduced aerial survey in 2017, and this report summarises the field procedures and data collected during the season. We describe the current methods for analysing the data (which have remained the same since 2012) and presents results from applying these methods to the data from all survey years.

3 Methods

3.1 Field procedures

The 2017 aerial survey was conducted in the GAB between 1 January and 31 March. One Rockwell Aero Commander 500S was chartered for the season. The plane contained an observer (spotter) that was calibrated into the survey in 2016. When flying along a line, the observer searched the sea surface from his side of the plane (the right side) through 180° to the other side of the plane (the left side) for surface patches (schools) of SBT.

The aerial survey continued to follow the protocols established for the 2000 survey (Cowling 2000) and used in all subsequent surveys with respect to the area searched, plane flying height and speed, minimum environmental conditions, time of day the survey lines were flown, and data recording protocols. Fifteen north-south transect lines (Figure 1) were surveyed. A complete replicate of the GAB consists of a subset of 12 (of the 15) lines divided into 4 blocks. In the past, the remaining 3 lines in a replicate (either: 1, 3 and 14, or 2, 13 and 15) were not searched, as SBT abundance was historically low in those areas and surveying a subset increases the number of complete replicates of the GAB in the survey. Over the past several years (since around 2009), however, the distribution of SBT in the GAB appears to have changed, with an increase in abundance in the eastern GAB compared to the western GAB (see Farley and Basson, 2013). Given this, lines 13, 14 and 15 were not routinely omitted on alternative replicates of the GAB.

The 2017 field operations were successful. Just over 5 replicates of the GAB were completed which is similar to the 3-5 replicates completed in previous years when only one plane was available, but lower than the 6-7 completed in 2010-2014 when two aircraft were available.

Figure 1. Location of the 15 north-south transect lines for the scientific aerial survey in the GAB.

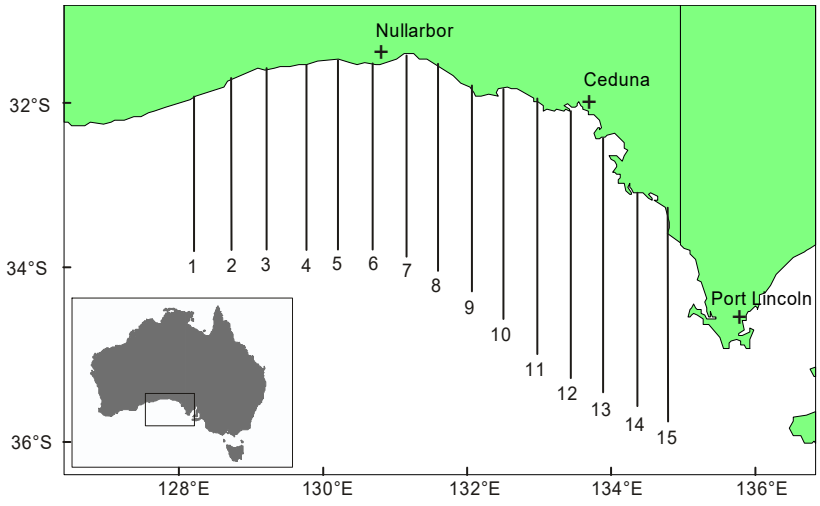

3.2 Data preparation

The data collected from the 2017 survey were loaded into the aerial survey database and checked for any obvious errors or inconsistencies and corrections made as necessary. In order for the

analyses to be comparable between all survey years, only data collected in a similar manner from a common area were included in the data summaries and analyses presented in this report. In particular, only search effort and sightings made along north/south transect lines in the unextended (pre-1999) survey area and sightings made within 6 nm of a transect line were included (see Basson et al. 2005 for details). In cases where a sighting consisted of more than one school, then the sighting was included if at least one of the schools was within 6 nm of the line. We excluded secondary sightings and any search distance and sightings made during the aborted section of a transect line (see Eveson et al. 2006 for details).

In the CCSBT operating model (OM) and management procedure (MP), the aerial survey index is assumed to provide a relative time series of age 2-4 abundance in the GAB. Thus, for consistency with the OM and MP as well as general consistency in interpretation of the index across years, schools estimated to be comprised of 1-year-old fish (i.e., that had an average fish size estimate of less than 8 kg) were omitted from the analysis. As described in Eveson et al. (2011), when two spotters are in a plane, they make independent estimates of the size of fish in each school, so we averaged their estimates to come up with a single estimate of average fish size. The percent of the total observed biomass coming from schools estimated to be comprised of fish less than 8 kg varies greatly between survey years (Table 1). This year, the estimate was 13.8%. This is much higher than in 2014 and 2016, but is still lower than the unusually high estimates obtained in 2010 to 2013.

Table 1. Percent of total biomass in each survey year coming from schools comprised of fish estimated to be less than 8kg on average (assumed to be 1-year-olds).

YEAR	%	YEAR	%
1993	0.2	2007	0.0
1994	7.4	2008	0.7
1995	8.8	2009	13.1
1996	3.7	2010	16.1
1997	8.2	2011	30.7
1998	6.2	2012	25.3
1999	1.4	2013	17.7
2000	0.8	2014	4.1
2005	2.1	2016	0.9
2006	0.7	2017	13.8

3.3 Search effort and sightings

A summary of the total search effort and SBT sightings made in each survey year is given in Table 2. All values are based on raw data, which have not been corrected for environmental factors or observer effects. This table, and all summary information and results presented in this report, include only the data specified in the previous section as being included in the analysis. Recall that schools comprised of fish less than 8 kg on average are omitted. Also note that the summary statistics include data from all flights, some of which had only one observer in 2010 and all of which had only one observer in 2011-2014 and 2017 (with the exception of two flights in 2012 and four flights in 2013).

The total distance searched in 2017 was similar to 2016, but lower than in any of the previous 5 surveys (2010-2014) due to the availability of only one survey plane. The raw sightings rate (number of sightings per 100 nm) and the size (average biomass) of the patches were close to average (Table 2; Fig. 2). However, the average number of patches per sighting was higher than in any previous survey, so the total biomass per nm was still relatively high (although markedly lower than the anomalously high value in 2016) (Table 2). ***Note that the statistics for 2010-2014 and 2017 include data from flights with only one observer, so caution must be used in comparing them directly with years for which all flights had two observers because we have shown previously that the sightings rate tends to be lower for flights with only one observer.***

Similar to 2016, the majority of sightings were made inshore and in the eastern half of the survey area (Fig. 3).

Table 2. Summary of aerial survey data by survey year. Only data considered suitable for analysis (as outlined in text) are included. All biomass statistics are in tonnes. All values in the table are based on raw data, which have not been corrected for environmental factors or observer effects.

SURVEY YEAR	TOTAL DISTANCE SEARCHED (NM)	NUMBER SBT SIGHTINGS	SIGHTINGS PER 100NM	TOTAL BIOMASS	BIOMASS PER NM	AVERAGE PATCHES PER SIGHTING	MAX PATCHES PER SIGHTING	AVERAGE BIOMASS PER PATCH	MAX BIOMASS PER PATCH
1993	7603	129	1.70	12219	1.61	4.0	76	24.5	203
1994	15180	160	1.05	13978	0.92	3.3	23	26.4	247
1995	14573	165	1.13	20149	1.38	3.5	38	34.7	225
1996	12284	110	0.90	16047	1.31	4.0	46	36.5	147
1997	8813	101	1.15	9154	1.04	3.2	18	28.5	203
1998	8550	104	1.22	9764	1.14	2.2	21	42.1	966
1999	7555	50	0.66	2998	0.40	2.5	21	24.2	122
2000	6775	76	1.12	4812	0.71	2.6	17	24.8	100
2005	5968	79	1.32	6043	1.01	2.4	17	32.1	198
2006	5150	43	0.83	4068	0.79	2.0	8	47.9	272
2007	4872	41	0.84	3538	0.73	2.6	11	33.4	123
2008	7462	121	1.62	8009	1.07	3.5	24	19.0	314
2009	8101	145	1.79	7964	0.98	2.5	22	22.3	172
2010[1]	10559	184	1.74	18477	1.75	4.0	41	24.9	539
2011[2]	10148	135	1.33	18559	1.83	2.7	37	50.2	400
2012[2]	10777	48	0.45	4939	0.46	3.2	45	32.1	507
2013[2]	12889	124	0.96	19127	1.48	3.0	18	52.0	634
2014[2]	12238	175	1.43	21213	1.73	2.4	25	49.7	481
2015	-	-	-	-	-	-	-	-	-
2016	7813	73	0.93	23931	3.06	3.8	28	86.1	714
2017	7784	73	0.94	13879	1.78	4.7	32	40.5	728

[1] Data comes from flights with one observer as well as flights with two observers.

[2] All data comes from flights with one observer (with the exception of one flight in 2012 and 3 flights in 2013).

Figure 2. Frequency of SBT patch sizes (in tonnes) by survey year.

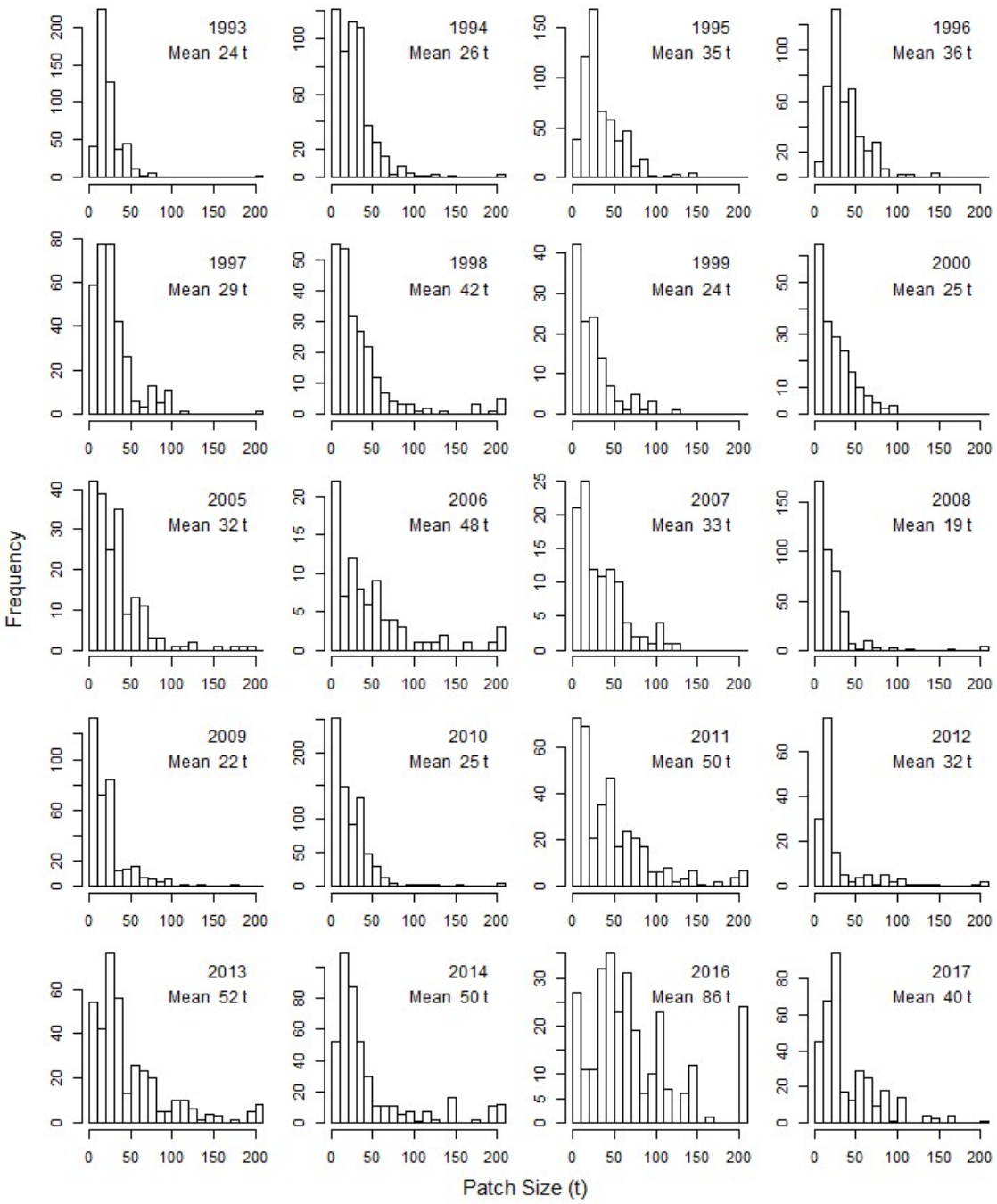

Figure 3. Distribution of SBT sightings made during each aerial survey year. Red circles show the locations of SBT sightings, where the size of the circle is proportional to the size of the sighting, and grey lines show the north/south transect lines that were searched.

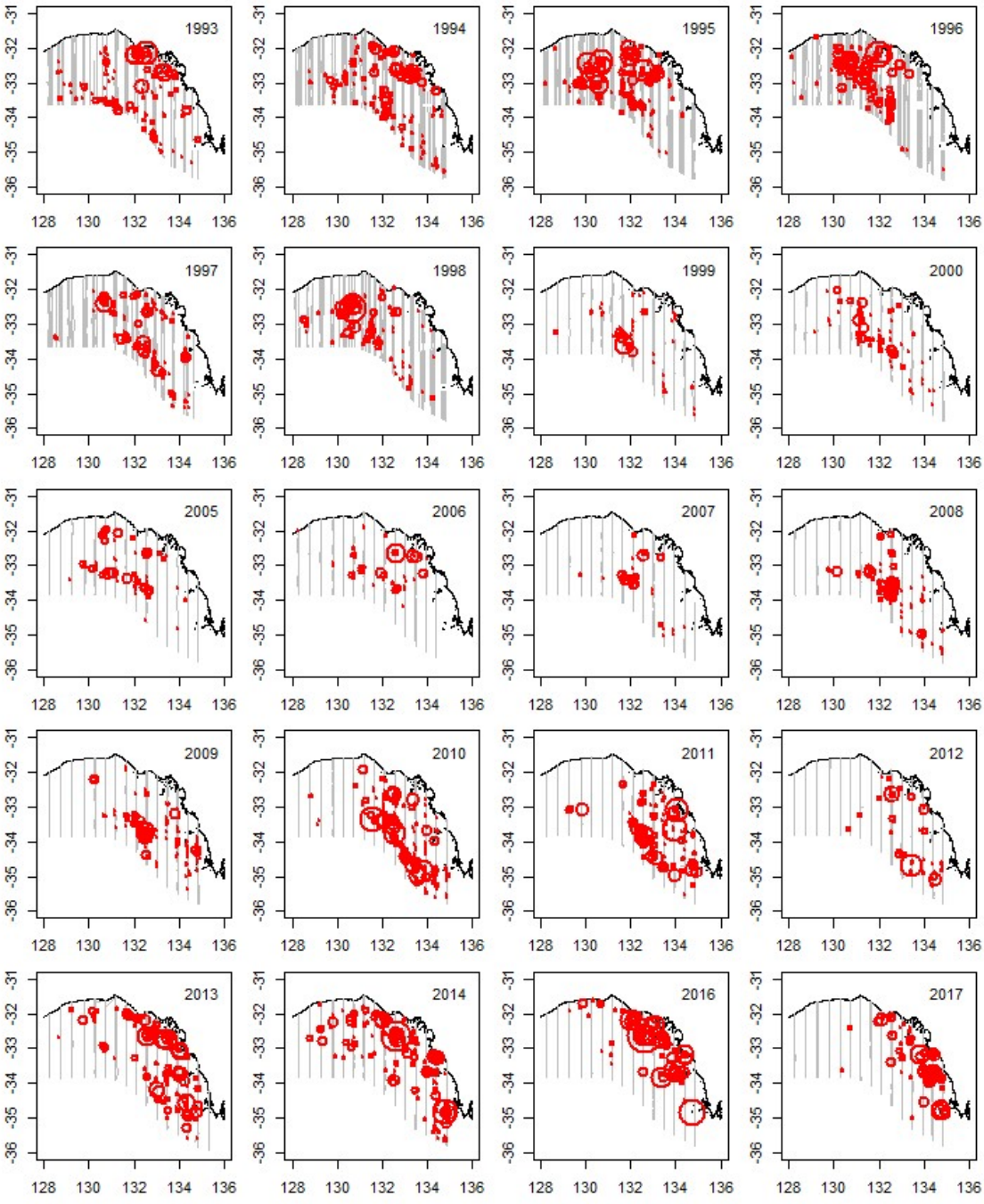

3.4 Environmental variables

Table 3 and Figure 4 summarize the environmental conditions that were present during valid search effort in each survey year. All the environmental variables presented were recorded by the survey plane(s), with the exception of sea surface temperature (SST), which was extracted from satellite remote sensing products. For all surveys up to and including 2014, the 3-day composite SST dataset produced by CSIRO Marine and Atmospheric Research's Remote Sensing Project was

used (see Eveson et al. 2006 for more details); however, this product stopped being available at the end of 2014 so was replaced with the Integrated Marine Observing System (IMOS) Group for High Resolution Sea Surface Temperature (GHRSST) (see http://imos.org.au/sstproducts.html).

The environmental conditions during the 2017 survey were close to average in terms of SST, sea shadow and haze; however, wind speed was lower than average and swell height was slightly higher than average (Table 3; Fig. 4). Increased wind speed tends to make it more difficult to observe surface schools whereas low swell tends to make it easier, so these variables will work in opposite directions in the standardization process to adjust the observed sightings rate to an average set of conditions.

Table 3. Average environmental conditions during search effort for each aerial survey year.

SURVEY YEAR	WIND SPEED (KNOTS)	SWELL HEIGHT (0-3)	AIR TEMP (°C)	SST (°C)	SEA SHADOW (0-8)	HAZE (0-3)
1993	3.9	0.8	24.4	19.6	1.9	0.9
1994	4.1	1.5	22.7	19.7	2.8	0.5
1995	4.4	1.7	18.7	19.6	2.7	1.1
1996	4.5	1.6	22.9	19.6	2.1	1.2
1997	4.1	1.7	25.3	21.1	1.6	1.3
1998	3.7	1.7	22.3	20.4	0.9	1.7
1999	4.1	0.9	22.0	19.9	2.9	0.7
2000	4.3	0.6	27.5	20.7	2.6	0.7
2005	4.7	1.5	21.7	20.1	1.6	0.8
2006	5.6	1.5	20.0	20.1	3.5	1.0
2007	5.8	1.3	21.6	20.8	2.0	1.3
2008	3.8	1.4	24.2	20.4	1.4	0.9
2009	3.8	1.4	22.3	21.0	2.2	1.7
2010	3.5	1.1	23.6	21.2	1.8	1.2
2011	3.9	1.3	20.2	20.3	2.8	1.4
2012	3.7	1.6	20.7	20.5	4.3	1.8
2013	4.2	1.6	24.6	21.7	2.6	1.6
2014	4.3	1.8	24.0	20.6	2.4	1.9
2016	4.1	1.8	20.5	20.3	4.1	0.9
2017	3.5	1.6	20.1	20.2	2.6	1.1

Figure 4. Boxplots summarizing the environmental conditions present during valid search effort for each aerial survey year. The thick horizontal band through a box indicates the median, the length of a box represents the inter-quartile range, and the vertical lines extend to the minimum and maximum values. The dashed blue line running across each plot shows the average across all survey years.

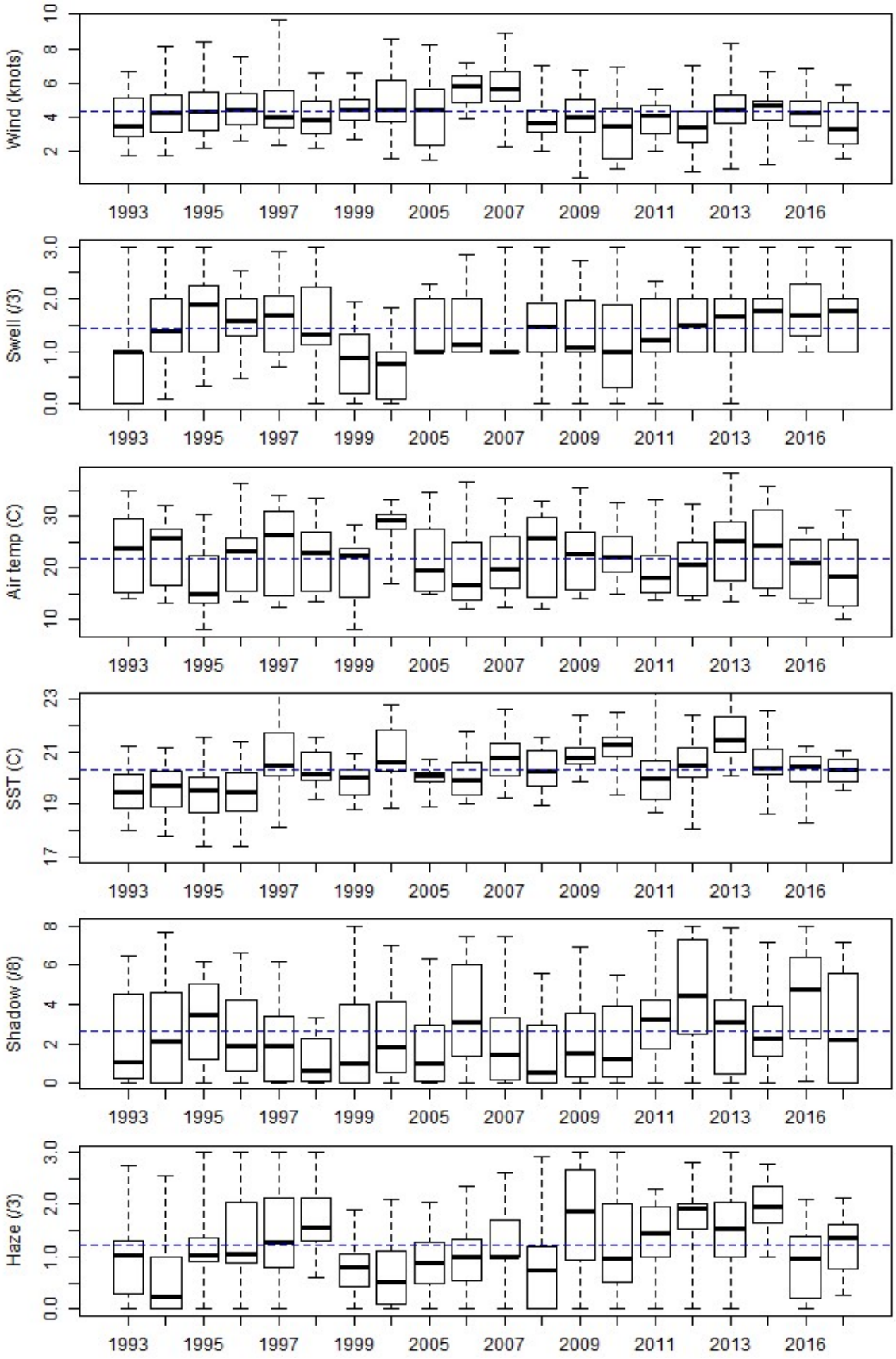

3.5 Method of analysis

The methods of analysis used this year were exactly the same as those used since 2012. A brief description of the methods is provided here and the details can be found in Appendix A.

Generalized linear models were fit to two different components of observed biomass—biomass per sighting (BpS) and sightings per nautical mile of transect line (SpM). The same environmental and observer variables were included in both models (noting that sea shadow was added to the SpM model last year). Specifically, the models can be expressed as:

BpS model: logE(Biomass) ~ Year*Month*Area + SST + WindSpeed

SpM model: logE(N_sightings) ~ offset{log(Distance) + log(ObsEffect)} + Year*Month*Area + SST + WindSpeed + Swell + Haze + MoonPhase + SeaShadow

As described in Appendix A, for the BpS model, we first need to estimate relative differences between observers in their estimates of school size in order to standardize the estimates for any consistent biases. In the past (e.g. Eveson et al. 2014), we have reported high consistency between observers, with school size estimates made by different observers tending to be within about 5% of a reference observer, except for one previous observer who tended to underestimate school sizes relative to the reference observer by about 20%. The spotter who flew in this year's survey tended to overestimate school sizes relative to the reference observer by about 10%. Recall that data from single-observer flights, which applies to this year's survey and the 2010 to 2014 surveys, can be included in the BpS model without any changes, except that there is only one biomass estimate per school so it is not necessary to take an average over the estimates made by two observers (refer to "Biomass per sighting (BpS) model" section in Appendix A).

Also described in Appendix A, for the SpM model, we first need to run a pairwise observer analysis based on within-flight comparisons of sighting rates to get estimates of the relative sighting efficiencies for all observer pairs that have flown at some point in the surveys. Past observer pairs have ranged in their estimated sighting efficiencies from 56% to 95% compared to the pair with the highest rate. For flights that only had a single observer, as was the case this year, we cannot get an estimated observer pair efficiency from this pairwise analysis. Instead, based on calibration experiments conducted in 2008 and 2009, we estimated that on average a plane with one observer will make about 70% as many sightings as a plane with two observers (Eveson et al. 2011). We refer to this factor as the "calibration factor". In order to estimate a relative sighting ability for a solo observer (i.e., an "observer effect"), we take the average of the relative sighting ability estimates from when this observer flew as part of a pair, and multiply it by the estimated calibration factor. For example, one of the observers who flew as a solo observer in the 2010 and 2011 surveys has flown as part of two different observer pairs in past surveys, with relative sighting ability estimates of 0.90 and 0.92. If we take the average of these two relative sighting ability estimates and multiply it by the calibration factor of 0.7, this gives a relative sighting ability estimate for this observer when flying solo of 0.64. This gives us "observer effect" estimates for all observer combinations, so we can proceed with fitting the SpM model in the usual way. For the observer in the 2017 survey, we estimate his observer effect when flying solo to be 0.44.

Note that, as of 2011, we include "observer effect" as an offset (i.e., as known) in the SpM model rather than as a linear covariate. The reason for this is discussed in Appendix A of Eveson et al. (2011). Because of this, we need to account for uncertainty in the observer effect estimates through other methods. Such methods have been developed for application to similar problems, but they are computer intensive and we have had difficulties implementing them successfully in this context. Thus, the standard errors, CVs and confidence intervals for the relative abundance

indices reported in Table 4 do not include uncertainty in the observer effects for the SpM model (meaning they are slight underestimates).

In both models, Year, Month and Area were fit as factors, as was MoonPhase in the SpM model. All other explanatory variables were fit as linear covariates. Note that the term Year*Month*Area encompasses all 1-way, 2-way and 3-way interactions between Year, Month and Area (i.e., it is equivalent to writing Year + Month + Area + Year:Month + Year:Area + Month:Area + Year:Month:Area).

In both models, the 2-way and 3-way interaction terms between Year, Month and Area were fit as random effects, whereas the 1-way effects were fit as fixed effects. Many of the 2-way and 3-way strata have very few (sometimes no) observations, which causes instabilities in the model fits when treated as fixed effects. One main advantage of using random effects is that when little or no data exist for a given level of a term (say for a particular area and month combination of the Area:Month term), we still have information about it because we are assuming it comes from a normal distribution with a certain mean and variance (estimated within the model).

Once the models were fitted, the results were used to predict what the number of sightings per mile and the average biomass per sighting in each of the 45 area/month strata in each survey year would have been under standardized environmental/observer conditions. Using these predicted values, we calculated an abundance estimate for each stratum as 'standardized SpM' multiplied by 'standardized average BpS'. We then took the weighted sum of the stratum-specific abundance estimates over all area/month strata within a year, where each estimate was weighted by the geographical size of the stratum in nm^2, to get an overall abundance estimate for that year. Lastly, the annual estimates were divided by their mean to get a time series of relative abundance indices.

We emphasise that it is important to have not only an estimate of the relative abundance index in each year, but also of the uncertainty in the estimates. We used the same process as in the last three years to calculate CVs for the indices, which takes into account the uncertainty in the calibration factor estimate. Details are provided in Appendix B. Recall from above that there is still uncertainty in the observer effect estimates for the SpM model, which is not currently being accounted for in the uncertainty estimates for the index.

We calculated confidence intervals for the indices based on the assumption that the logarithm of the indices follows a normal distribution, with standard errors approximated by the CVs of the untransformed indices.

4 Results

Figure 5 shows the estimated time series of relative abundance indices with 90% confidence intervals. The point estimates and CVs corresponding to Figure 5 are given in Table 4. Recall from the Methods section that all of the confidence intervals are being slightly underestimated because they do not account for uncertainty in the observer effect estimates.

The 2017 point-estimate is similar to the 2014 estimate, and significantly above the long-term average when taking confidence intervals into account. Although it is markedly lower than the 2016 estimate, the 2016 estimate was anomalously high.

(Results and diagnostics for the BpS and SpM models are provided in Appendix C.)

Figure 5. Time series of relative abundance estimates with 90% confidence intervals.

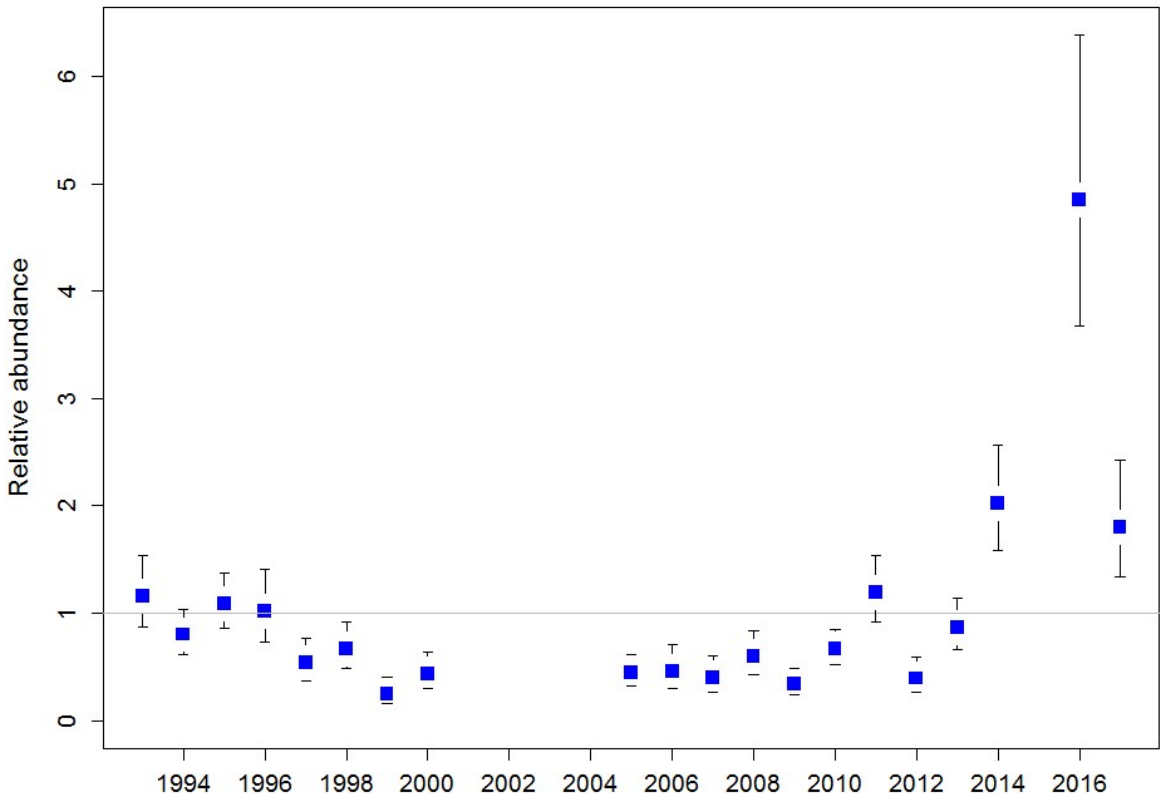

Table 4. Results from the aerial survey analysis.

YEAR	INDEX	SE	CV	CI.05	CI.95
1993	1.16	0.20	0.17	0.88	1.53
1994	0.80	0.13	0.16	0.62	1.04
1995	1.09	0.16	0.14	0.86	1.38
1996	1.02	0.20	0.20	0.74	1.41
1997	0.54	0.12	0.22	0.38	0.77
1998	0.67	0.13	0.20	0.49	0.92
1999	0.25	0.07	0.28	0.16	0.40
2000	0.44	0.10	0.23	0.30	0.64
2005	0.45	0.09	0.19	0.33	0.61
2006	0.46	0.12	0.26	0.30	0.71
2007	0.40	0.10	0.25	0.27	0.60
2008	0.60	0.12	0.21	0.43	0.84
2009	0.34	0.07	0.22	0.24	0.49
2010	0.67	0.10	0.15	0.53	0.85
2011	1.20	0.19	0.16	0.93	1.54
2012	0.39	0.10	0.24	0.26	0.59
2013	0.87	0.14	0.17	0.66	1.14
2014	2.02	0.29	0.15	1.59	2.56
2016	4.85	0.81	0.17	3.68	6.38
2017	1.80	0.33	0.18	1.34	2.42

Index = relative abundance point estimates; SE= standard error; CV = coefficient of variation; CI.05 and CI.95 = lower and upper range of 90% confidence interval.

5 Summary

The estimate of relative juvenile abundance from the 2017 scientific aerial survey is similar to the 2014 estimate, and significantly above the long-term average. Although it is much lower than the 2016 estimate, the 2016 estimate was anomalously high. The survey was not conducted in 2015 due to a lack of agreement about funding, so we do not have an estimate for that year for comparison.

The methods of analysis used this year were the same as those used since 2012. The CVs for the relative abundance indices do not include uncertainty in the observer effects for the SpM model, so they will be slightly underestimated.

The environmental conditions during the 2017 survey were average for the most part, except that wind speed tended to be lower and swell height slightly higher than the long-term average. Similar to 2016, most sightings were made inshore in the eastern half of the survey area. As in 2009-2013, a high percentage of the observed total biomass coming from schools comprised of small fish (<8 kg) was observed again this year (13.8%).

6 References

Anonymous. 2008. Report of the Thirteenth Meeting of the Scientific Committee, Commission for the Conservation of Southern Bluefin Tuna, 5-12 September 2008, Rotorua, New Zealand.

Basson, M., Bravington, M., Eveson, P. and Farley, J. 2005. Southern bluefin tuna recruitment monitoring program 2004-05: Preliminary results of Aerial Survey and Commercial Spotting data. Final Report to DAFF, June 2005.

Bravington, M. 2003. Further considerations on the analysis and design of aerial surveys for juvenile SBT in the Great Australian Bight. RMWS/03/03.

Cowling, A. 2000. Data analysis of the aerial surveys (1993-2000) for juvenile southern bluefin tuna in the Great Australian Bight. RMWS/00/03.

Cowling A., Hobday, A., and Gunn, J. 2002. Development of a fishery independent index of abundance for juvenile southern bluefin tuna and improvement of the index through integration of environmental, archival tag and aerial survey data. FRDC Final Report 96/111 and 99/105.

Eveson, P., Bravington, M. and Farley, J. 2006. The aerial survey index of abundance: updated analysis methods and results. CCSBT-ESC/0609/16.

Eveson, P., Bravington, M. and Farley, J. 2007. Aerial survey: updated index of abundance and preliminary results from calibration experiment. CCSBT-ESC/0709/12.

Eveson, P., Bravington, M. and Farley, J. 2008. The aerial survey index of abundance: updated analysis methods and results. CCSBT-ESC/0809/24.

Eveson, P., Farley, J., and Bravington, M. 2009. The aerial survey index of abundance: updated analysis methods and results. CCSBT-ESC/0909/12.

Eveson, P., Farley, J., and Bravington, M. 2010. The aerial survey index of abundance: updated analysis methods and results for the 2009/10 fishing season. CCSBT-ESC/1009/14.

Eveson, P., Farley, J., and Bravington, M. 2011. The aerial survey index of abundance: updated analysis methods and results for the 2010/11 fishing season. CCSBT-ESC/1107/15.

Eveson, P., Farley, J., and Bravington, M. 2014. The aerial survey index of abundance: updated results for the 2013/14 fishing season. CCSBT-ESC/1409/18.

Eveson P, Farley J. 2016. The aerial survey index of abundance: 2016 updated results. CCSBT-ESC/1609/09.

Appendix A - Methods of analysis

Separate models were constructed to describe two different components of observed biomass: i) biomass per patch sighting (BpS) and ii) sightings per nautical mile of transect line (SpM). Each component was fitted using a generalized linear mixed model (GLMM), as described below. Since environmental conditions affect what proportion of tuna are available at the surface to be seen, as well as how visible those tuna are, and since different observers can vary both in their estimation of school size and in their ability to see tuna patches, the models include 'corrections' for environmental and observer effects in order to produce standardized indices that can be meaningfully compared across years.

For the purposes of analysis, we defined 45 area/month strata: 15 areas (5 longitude blocks and 3 latitude blocks, as shown in Figure A1) and 3 months (Jan, Feb, Mar). The latitudinal divisions were chosen to correspond roughly to depth strata (inshore, mid-shore and shelf-break).

Figure A1. Plot showing the 15 areas (5 longitudinal bands and 3 latitudinal bands) into which the aerial survey is divided for analysis purposes. The green vertical lines show the official transect lines for the surveys conducted in 1999 and onwards; the lines for previous survey years are similar but are slightly more variable in their longitudinal positions and also do not extend quite as far south (which is why the areas defined for analysis, which are common to all survey years, do not extend further south).

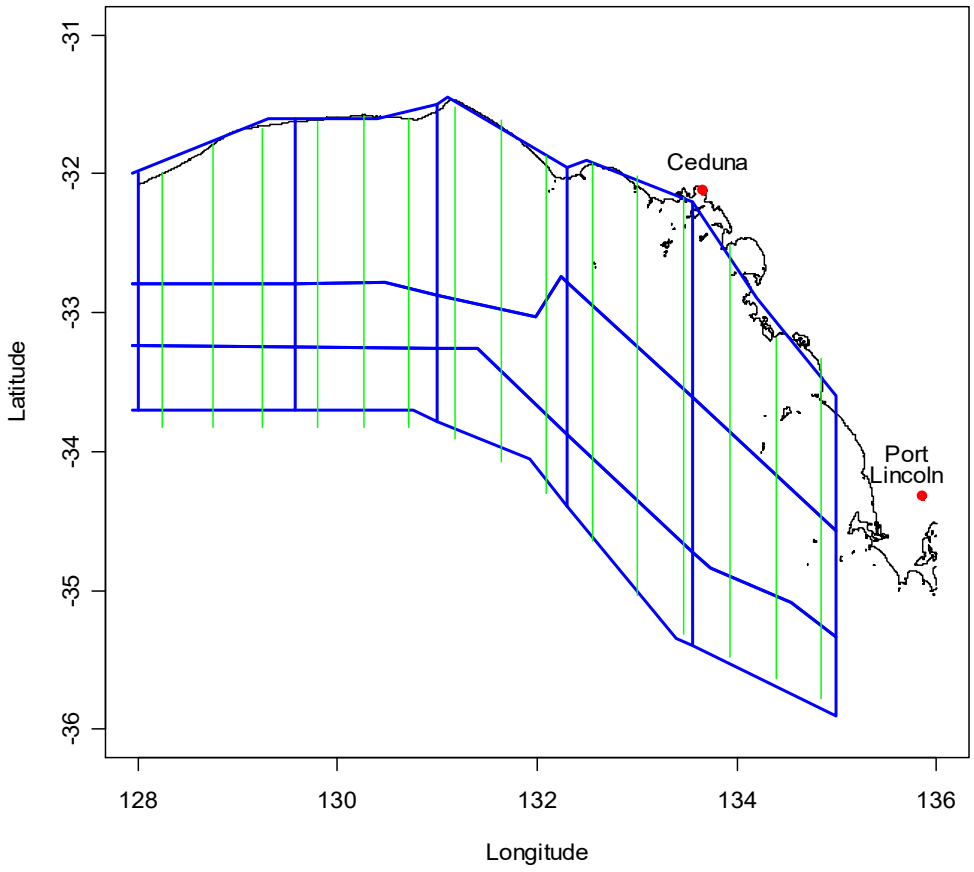

A.1 Biomass per sighting (BpS) model

For the BpS model, we first estimated relative differences between observers in their estimates of patch size (using the same methods as described in Bravington 2003). As in Bravington (2003), we

found good consistency between observers. In particular, patch size estimates made by different observers tended to be within about 5% of each other, except for two observers, say X and Y, where X tended to underestimate patch sizes relative to other observers by about 20%, and Y tended to overestimate them by about 10%. The patch size estimates were corrected using the estimated observer differences (e.g. patch size estimates made by observer X were scaled up by 20%, and those made by Y were scaled down by 10%).Because the observer differences were estimated with high precision, we treated the corrected patch size estimates as exact in our subsequent analyses. The final biomass estimate for each patch was calculated as the average of the two corrected estimates (recall that the size of a patch is estimated by both observers in the plane). The final patch size estimates were then aggregated within sightings to give an estimate of the total biomass of each sighting. It is the total biomass per sighting data that are used in the BpS model.

The BpS model was fitted using a GLMM with a log link and a Gamma error structure. We chose to fit a rather rich model with 3-way interaction terms between year, month and area. This is true not only for the BpS model but also for the SpM model described below. In essence, the 3-way interaction model simply corrects the observation (the total biomass of a sighting in the case of the BpS model; the number of sightings in the case of the SpM model) for environmental effects, which are estimated from within-stratum comparisons (i.e. within each combination of year, month and area).

The 2-way and 3-way interaction terms between Year, Month and Area were fit as random effects, whereas the 1-way effects were fit as fixed effects. Many of the 2-way and 3-way strata have very few (sometimes no) observations, which causes instabilities in the model fits when treated as fixed effects. One main advantage of using random effects is that when little or no data exist for a given level of a term (say for a particular area and month combination of the Area:Month term), we still have information about it because we are assuming it comes from a normal distribution with a certain mean and variance (estimated within the model).

Based on exploratory plots and model fits, we confirmed that SST has a significant effect on the biomass per sighting, and that wind speed has a lesser but still significant effect (p-value 0.02; see Appendix C.1). Thus, the final model fitted was

$$\log E(\text{Biomass}) \sim \text{Year}*\text{Month}*\text{Area} + \text{SST} + \text{WindSpeed}$$

where Year, Month and Area are factors, and SST and WindSpeed are linear covariates (note that E is standard statistical notation for expected value).

A.2 Sightings per mile (SpM) model

For the SpM model, we first ran the pairwise observer analysis described in Bravington (2003), based on within-flight comparisons of sighting rates between the various observers. This analysis gives estimates of the relative sighting efficiencies for all of the different observer pairs that have flown at some point in the surveys. The observer pairs ranged in their estimated sighting efficiencies from 56% to 95% compared to the pair with the best rate. For the observers that flew alone in the 2010-2014 and 2017 surveys, their “observer effect” estimate (as described in the Methods section of the main text) ranged from 44% to 66% (again relative to the observer pair with the best rate).

We include the (logged) estimates of relative observer pair efficiencies as an offset when fitting the SpM model (i.e., as a predictor variable with a known, rather than estimated, coefficient). Appendix A of Eveson et al. 2011 discusses this in more detail. As such, we need to account for the uncertainty in these estimates through other methods. Such methods have been developed for other applications but have proven difficult to implement in this context. Thus, the standard errors and CVs for the relative abundance indices reported in Table 4 do not include uncertainty in the observer effects for the SpM model (which means they are slightly too small).

The data used for the SpM model were accumulated by flight and area, so that the data set used in the analysis contains a row for every flight/area combination in which search effort was made (even if no sightings were made). Within each flight/area combination, the number of sightings and the distance flown were summed, whereas the environmental conditions were averaged. The SpM model was fitted using a GLMM with the number of sightings as the response variable, as opposed to the sightings rate. The model could then be fitted assuming an overdispersed Poisson error structure[3] with a log link and including the distance flown as an offset term to the model (i.e. as a linear predictor with a known coefficient of one).

As we did for the BpS model, we included terms for year, month and area, as well as all possible interactions between them, in the SpM model, and we fitted the 2-way and 3-way interaction terms as random effects (see BpS model section). We determined what environmental variables to include in the model based on exploratory plots and model fits. The final model fitted was:

logE(N_sightings) ~ offset(log(Distance) + log(ObsEffect)) + Year*Month*Area + SST + WindSpeed + Swell + Haze + MoonPhase + SeaShadow

where Year, Month and Area are factors, MoonPhase is a factor (taking on one of four levels from new moon to full moon), and all other terms are linear covariates. Note that MoonPhase is no longer coming out significant (see Appendix C.2) but we chose to keep it in the model for consistency with previous years.

A.3 Combined analysis

The BpS and SpM model results were used to predict what the number of sightings per mile and the average biomass per sighting in each of the 45 area/month strata in each survey year would have been under standardized environmental/observer conditions[4]. Using these predicted values, we calculated an abundance estimate for each stratum as 'standardized SpM' multiplied by 'standardized average BpS'. We then took the weighted sum of the stratum-specific abundance estimates over all area/month strata within a year, where each estimate was weighted by the geographical size of the stratum in nm^2, to get an overall abundance estimate for that year. Lastly, the annual estimates were divided by their mean to get a time series of relative abundance indices.

[3] Note that the standard Poisson distribution has a very strict variance structure in which the variance is equal to the mean, and it would almost certainly underestimate the amount of variance in the sightings data, hence the use of an overdispersed Poisson distribution to describe the error structure.

[4] In our predictions, we used average conditions calculated from all the data.

Appendix B - CV calculations

This appendix provides details of how CVs for the aerial survey abundance indices were calculated.

Let $\hat{B}_{ijk}$ be the predicted value of BpS in year *i*, month *j* and area *k* under standardized environmental/observer conditions (see footnote 4), and $\hat{\sigma}\left(\hat{B}_{ijk}\right)$ be its estimated standard error. Similarly, let $\hat{S}_{ijk}$ be the predicted value of SpM in year *i*, month *j* and area *k* under the same environmental/observer conditions, and $\hat{\sigma}\left(\hat{S}_{ijk}\right)$ be its estimated standard error. Then,

$$\hat{A}_{ijk} = \hat{S}_{ijk}\hat{B}_{ijk}$$

is the stratum-specific abundance estimate for year *i*, month *j* and area *k*.

Since $\hat{B}_{ijk}$ and $\hat{S}_{ijk}$ are independent, the variance of $\hat{A}_{ijk}$ is given by

$$\begin{aligned} V\left(\hat{A}_{ijk}\right) &= V\left(\hat{S}_{ijk}\hat{B}_{ijk}\right) \\ &= V\left(\hat{S}_{ijk}\right)E\left(\hat{B}_{ijk}\right)^2 + V\left(\hat{B}_{ijk}\right)E\left(\hat{S}_{ijk}\right)^2 + V\left(\hat{S}_{ijk}\right)V\left(\hat{B}_{ijk}\right) \\ &\approx \hat{\sigma}^2\left(\hat{S}_{ijk}\right)\hat{B}_{ijk}{}^2 + \hat{\sigma}^2\left(\hat{B}_{ijk}\right)\hat{S}_{ijk}{}^2 + \hat{\sigma}^2\left(\hat{S}_{ijk}\right)\hat{\sigma}^2\left(\hat{B}_{ijk}\right) \end{aligned}$$

The annual abundance estimate for year *i* is given by the weighted sum of all stratum-specific abundance estimates within the year, namely

$$\hat{A}_i = \sum_j \sum_k w_k \hat{A}_{ijk}$$

where w_k is the proportional size of area *k* relative to the entire survey area ($\sum_k w_k = 1$).

If the $\hat{A}_{ijk}$'s are independent, then the variance of $\hat{A}_i$ is given by

$$V\left(\hat{A}_i\right) = \sum_j \sum_k w_k{}^2 V\left(\hat{A}_{ijk}\right)$$

Unfortunately, the $\hat{A}_{ijk}$'s are NOT independent because the estimates of BpS (and likewise, the estimates of SpM) are not independent between different strata. This is because all strata estimates depend on the estimated coefficients of the environmental/observer conditions, so any error in these estimated coefficients will affect all strata. Thus, we refit the BpS and SpM models with the coefficients of the environmental/observer covariates (denote the vector of coefficients

by θ[5]) fixed at their estimated values ($\hat{\theta}$). The predictions of BpS and SpM made using the 'fixed environment' models should now be independent between strata, so the stratum-specific abundance estimates calculated using these predictions – which we will denote by $\hat{A}_{ijk}\left(\hat{\theta}\right)$ – should also be independent between strata. Thus, we can calculate the variance of $\hat{A}_i$ conditional on the estimated values of the environmental/observer coefficients as

$$V\left(\hat{A}_i \mid \hat{\theta}\right) = \sum_j \sum_k w_k{}^2 V\left(\hat{A}_{ijk}\left(\hat{\theta}\right)\right)$$

where $V\left(\hat{A}_{ijk}\left(\hat{\theta}\right)\right)$ is calculated using the formula given above for $V\left(\hat{A}_{ijk}\right)$ but using the BpS and SpM predictions and standard errors obtained from the 'fixed environment' models.

To calculate the unconditional variance of $\hat{A}_i$, we make use of the following equation:

$$\begin{aligned} V\left(\hat{A}_i\right) &= E_\theta\left(V\left(\hat{A}_i \mid \theta\right)\right) + V_\theta\left(E\left(\hat{A}_i \mid \theta\right)\right) \\ &\approx V\left(\hat{A}_i \mid \hat{\theta}\right) + V_\theta\left(\hat{A}_i\right) \end{aligned}$$

where the first term is the conditional variance just discussed and the second term is the additional variance due to uncertainty in the environmental coefficients. The second term can be estimated as follows

$$V_\theta\left(\hat{A}_i\right) \approx \left(\frac{\partial \hat{A}_i}{\partial \theta}\right)' \mathbf{V}_\theta \left(\frac{\partial \hat{A}_i}{\partial \theta}\right)$$

where $\left(\frac{\partial \hat{A}_i}{\partial \theta}\right)$ is the vector of partial derivatives of $\hat{A}_i$ with respect to θ (which we calculated using numerical differentiation), and $\mathbf{V}_\theta$ is the variance-covariance matrix of the environmental coefficients[6].

Now, to account for the additional variance due to uncertainty in the calibration factor, we use a similar approach as above to account for additional variance due to uncertainty in the environmental coefficients. Namely, from the GLM used to estimate the calibration factor, which we will call α, we get an estimate of its variance, which we will call V_α. Then, the variance in the abundance estimates due to uncertainty in α can be estimated by

---

[5] θ contains the environmental/observer coefficients from both the BpS and SpM models; i.e. $\theta = (\theta_{\text{BpS}}, \theta_{\text{SpM}})$

[6] Recall that θ contains the environmental/observer coefficients from both the BpS and SpM models, so $\mathbf{V}_\theta = \begin{bmatrix} \mathbf{V}_{\theta_{\text{BpS}}} & \mathbf{0} \\ \mathbf{0} & \mathbf{V}_{\theta_{\text{SpM}}} \end{bmatrix}$. The variance-covariance matrices for the individual models are returned from the model-fitting software.

$$V_\alpha\left(\hat{A}_i\right)=\left(\frac{\partial\hat{A}_i}{\partial\alpha}\right)' V_\alpha\left(\frac{\partial\hat{A}_i}{\partial\alpha}\right)$$

where $\left(\frac{\partial\hat{A}_i}{\partial\alpha}\right)$ is the derivative of $\hat{A}_i$ with respect to α (in essence, it is the amount that the abundance estimate $\hat{A}_i$ changes when the calibration factor is tweaked slightly). Thus, we revise our estimate of $V\left(\hat{A}_i\right)$ by adding on to it $V_\alpha\left(\hat{A}_i\right)$.

So we have variance estimates for the abundance estimates, but we also want to calculate the variance for the mean-standardized estimates (referred to as the relative abundance indices), calculated as:

$$\hat{I}_i=\frac{\hat{A}_i}{\frac{1}{n}\sum_{i=1}^{n}\hat{A}_i}$$

Using the delta method, we can approximate the variance of $\hat{I}_i$ by

$$V\left(\hat{I}_i\right)\approx\left(\frac{\partial\hat{I}_i}{\partial\hat{A}_i}\right)^2 V\left(\hat{A}_i\right)$$

Then, the standard error of $\hat{I}_i$ is given by

$$\sigma\left(\hat{I}_i\right)=\sqrt{V\left(\hat{I}_i\right)}$$

and the coefficient of variation (CV) of $\hat{I}_i$ is given by

$$\mathrm{CV}\left(\hat{I}_i\right)=\frac{\sigma\left(\hat{I}_i\right)}{\hat{I}_i}.$$

Appendix C - Results and diagnostics

A.4 Biomass per sighting (BpS) model

Figure C1 shows plots of observed biomass per sighting (logged) versus the environmental covariates being included in the BpS model. From these plots, it appears that the size of a sighting tends to increase as SST increases, and possibly decrease as wind speed increases (in a roughly linear fashion in both cases when on a log scale). The relationship with SST appears to be strongest, as supported by the model results (below).

Extract from the output produced by the software used to fit the model (the gam function in the R statistical package mgcv):

```
Family: Gamma
Link function: log

Formula:
Biomass ~ factor(Year) + factor(Month) + factor(Area) + SST + WindSpeed +
Y.M + Y.A + M.A + Y.M.A - 1
```

Parametric Terms:

Covariate	Estimate	SE	t-value	p-value
SST	0.108	0.036	3.02	0.003
WindSpeed	-0.056	0.022	-2.58	0.010

```
R-sq.(adj) =  0.116   Deviance explained = 38.1%
GCV score =  1.9368  Scale est. = 1.7074    n = 2130
```

The results support our observations made based on Figure C1; size of a sighting tends to increase as SST increases and decrease as wind speed increases, but that the relationship with SST has greater statistical significance.

Figure C2 shows some standard diagnostic plots for generalized linear models, and Figure C3 shows the residuals plotted against a number of factors. These plots do not suggest major problems with the model fit. Ideally there should be no trend in the plots of the square root of the absolute residuals against the fitted values (i.e., lower half of Fig. C2, with left-hand side being on the link scale and the right-hand side being on the response scale); although there is a small kink revealed by a smooth through the data (red line), there is not a consistent increasing or decreasing trend.

Figure C1. Plots of observed biomass per sighting, on a log scale, versus the covariates included in the model; shown is the mean +/- 2 standard deviations.

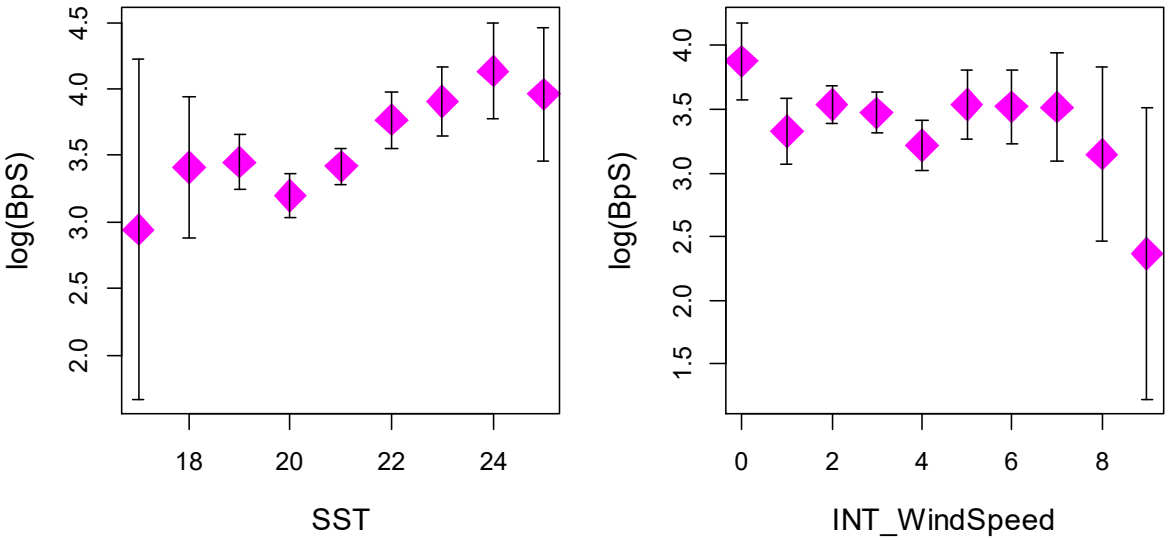

Figure C2. Standard diagnostic plots for biomass per sighting (BpS) model.

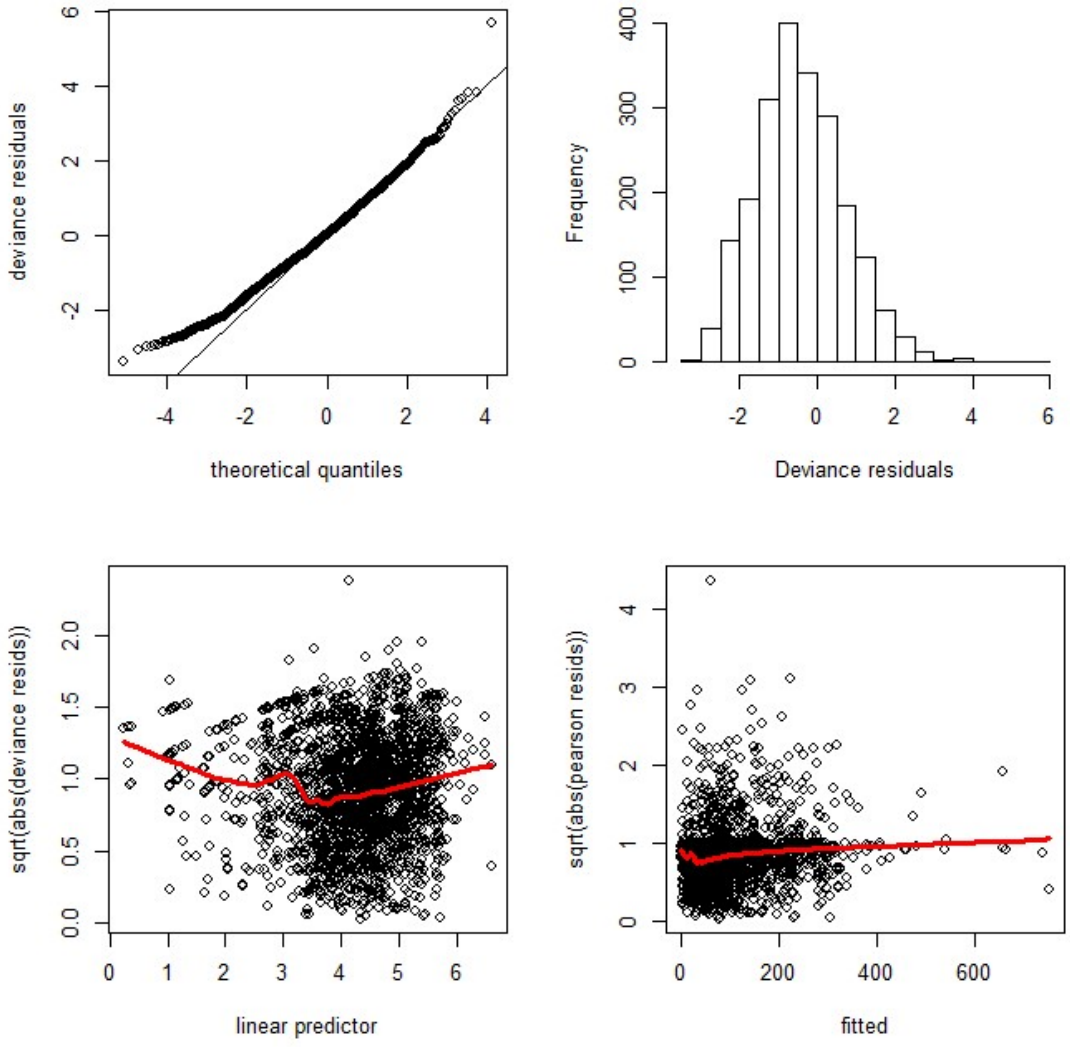

Figure C3. Boxplots of deviance residuals by year, month and area for biomass per sighting (BpS) model.

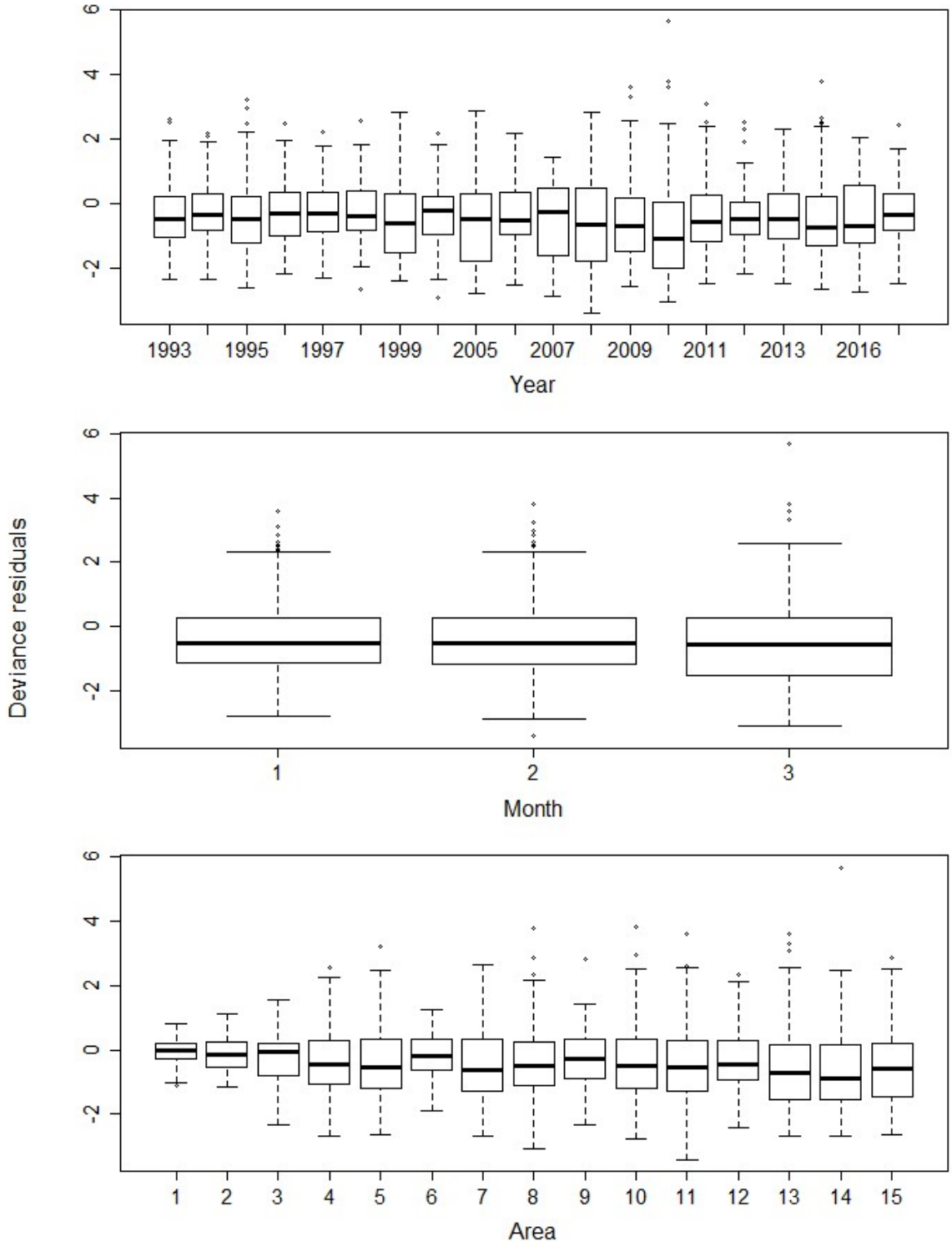

A.5 Sightings per mile (SpM) model

Figure C4 shows plots of observed number of sightings per mile (logged) versus the environmental covariates being included in the SpM model. There appears to be a strong tendency for the rate of sightings to increase as SST increases, and to decline as wind speed, haze, swell and sea shadow increase. With the exception of wind speed, the relationship appears to be linear, and this is even true for wind speed in the range of 1 to 7 knots (where most of the observations occur). Moon phase also appears to influence the sightings rate, with the rate being greatest when the moon phase is 1 (fraction of moon illuminated is 0-25%) or 4 (fraction of moon illumination is 75-100%), but the variance is large so the relationship may not be statistically significant.

Extract from the output produced by the software used to fit the model (the gam function in the R statistical package mgcv):

```
Family: quasipoisson
Link function: log

Formula:
N_sightings ~ offset(log(as.numeric(Distance))) + factor(Year) +
factor(Month) + factor(Area) + Y.M + Y.A + M.A + Y.M.A +
log(ObserverEffect) + AvgWindSpeed + AvgSST + AvgSwell + AvgHaze +
factor(MoonPhase) - 1

Parametric Terms:
```

Covariate	Estimate	SE	t-value	p-value
AvgWindSpeed	-0.271	0.020	-13.878	0.000
AvgSST	0.184	0.031	5.904	0.000
AvgSwell	-0.185	0.047	-3.936	0.000
AvgHaze	-0.143	0.041	-3.451	0.001
AvgSeaShadow	-0.077	0.013	-5.734	0.000
factor(MoonPhase)2	-0.086	0.084	-1.032	0.302
factor(MoonPhase)3	-0.059	0.104	-0.572	0.567
factor(MoonPhase)4	0.070	0.070	0.990	0.322

```
R-sq.(adj) =  0.501   Deviance explained = 67.8%
GCV score = 1.3436  Scale est. = 1.0954    n = 2337
```

The results again suggest that there is a tendency for the rate of sightings to increase as SST increases, and to decline as wind speed, haze, swell and sea shadow increase (all highly significant). The relationship with moon phase is no longer coming out significant at the 0.05 level, but we retain it in the model for consistency with previous years.

Figure C5 shows some standard diagnostic plots for generalized linear models, and Figure C6 shows the residuals plotted against a number of factors. The Q-Q plot (top left) suggests lack of fit at the tails of the distribution, which is common; however it also has a strange kink in the centre. Otherwise there are no indications of serious problems with the model fit. The plots of the square root of the absolute residuals against the fitted values (i.e., lower half of Fig. C5, with left-hand side being on the link scale and the right-hand side being on the response scale) look a bit odd, but this is expected because we are modelling count data. A smooth line through these data is reasonably flat, as desired, except for where it follows the residuals for the zero response values (i.e., where the observed number of sightings was zero).

Figure C4. Plots of observed sightings per mile, on a log scale, versus the covariates included in the model; shown is the mean +/- 2 standard deviations.

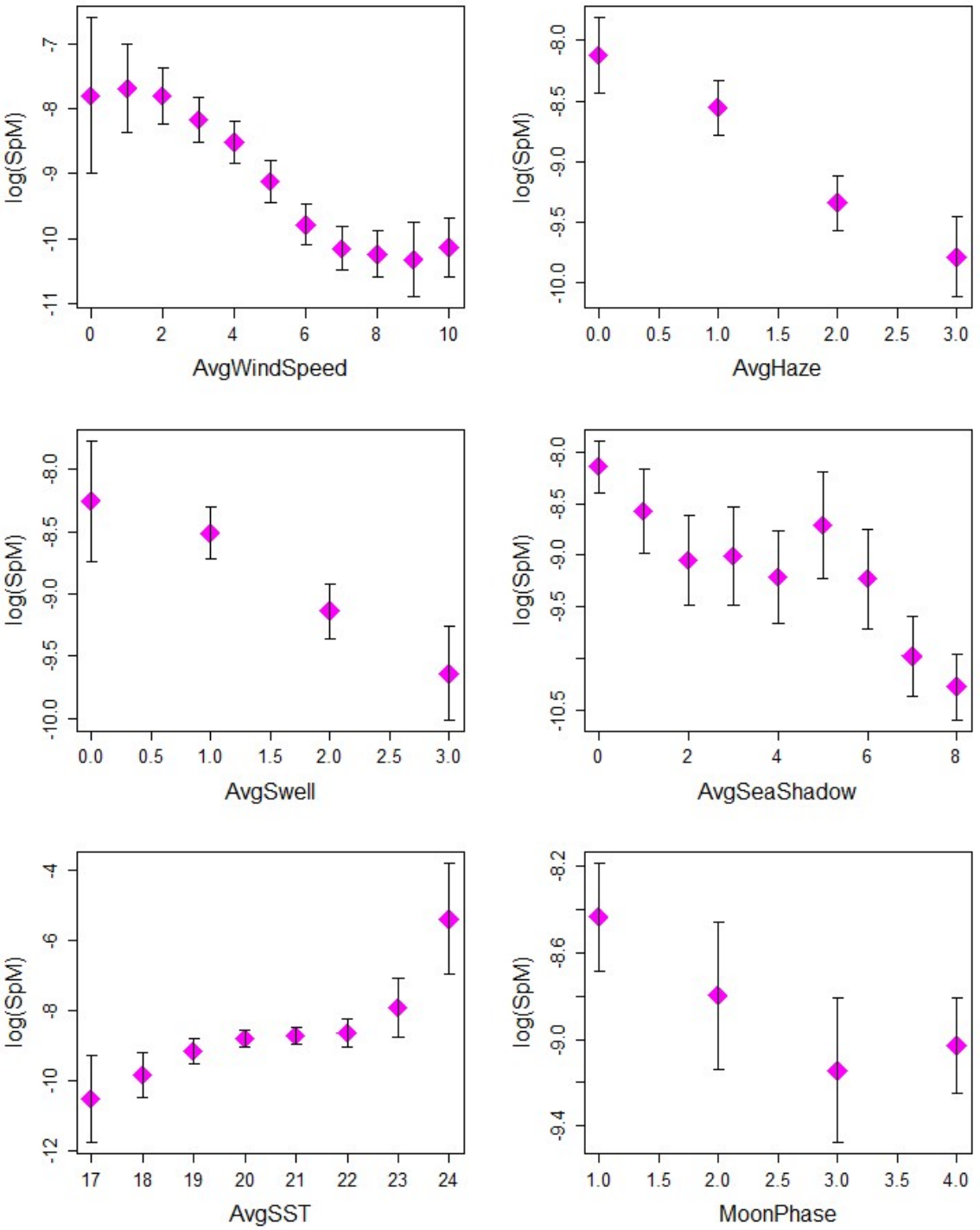

Figure C5. Standard diagnostics plots for sightings per mile (SpM) model.

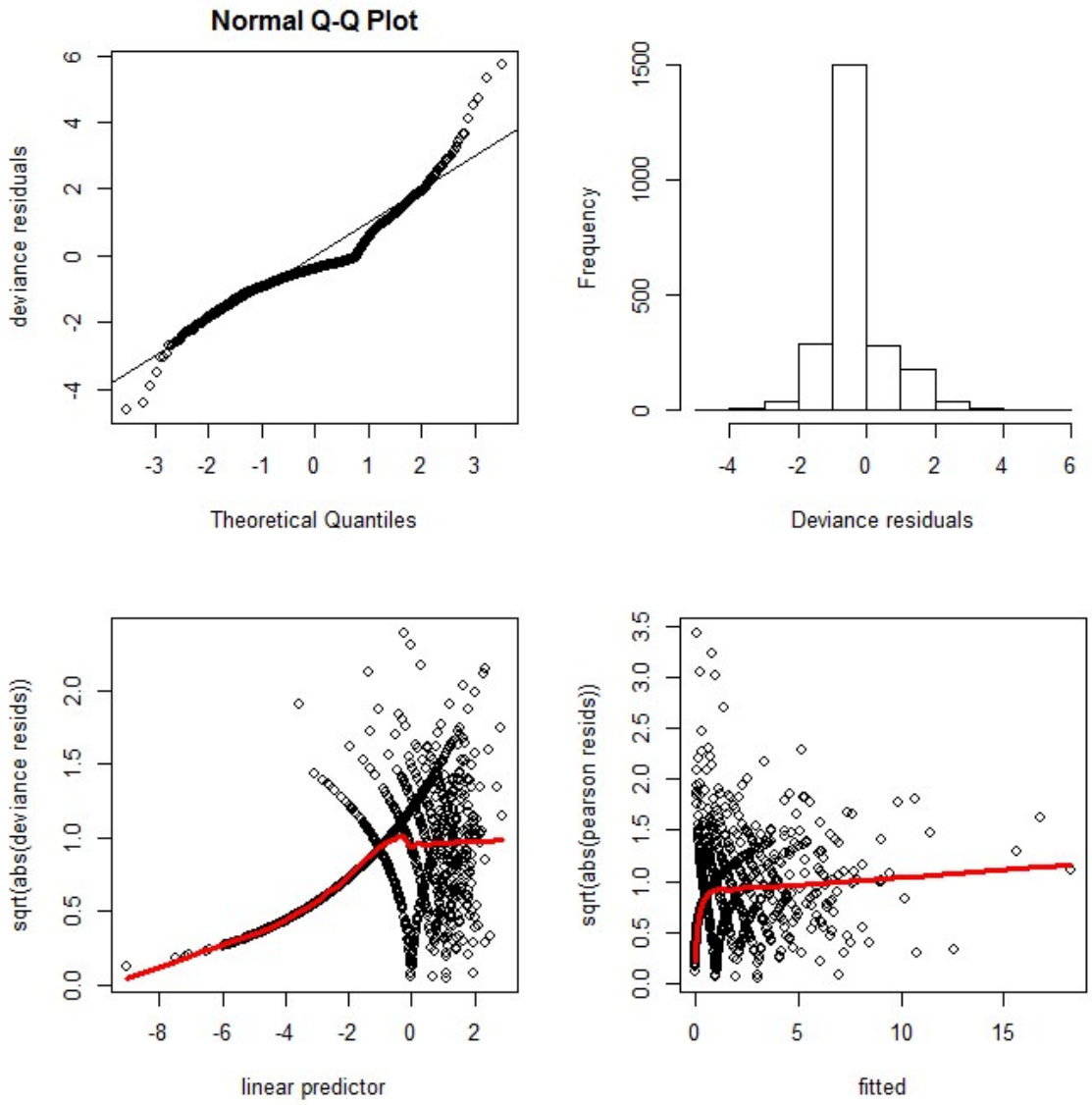

Figure C6. Boxplots of deviance residuals by year, month and area for sightings per mile (SpM) model.

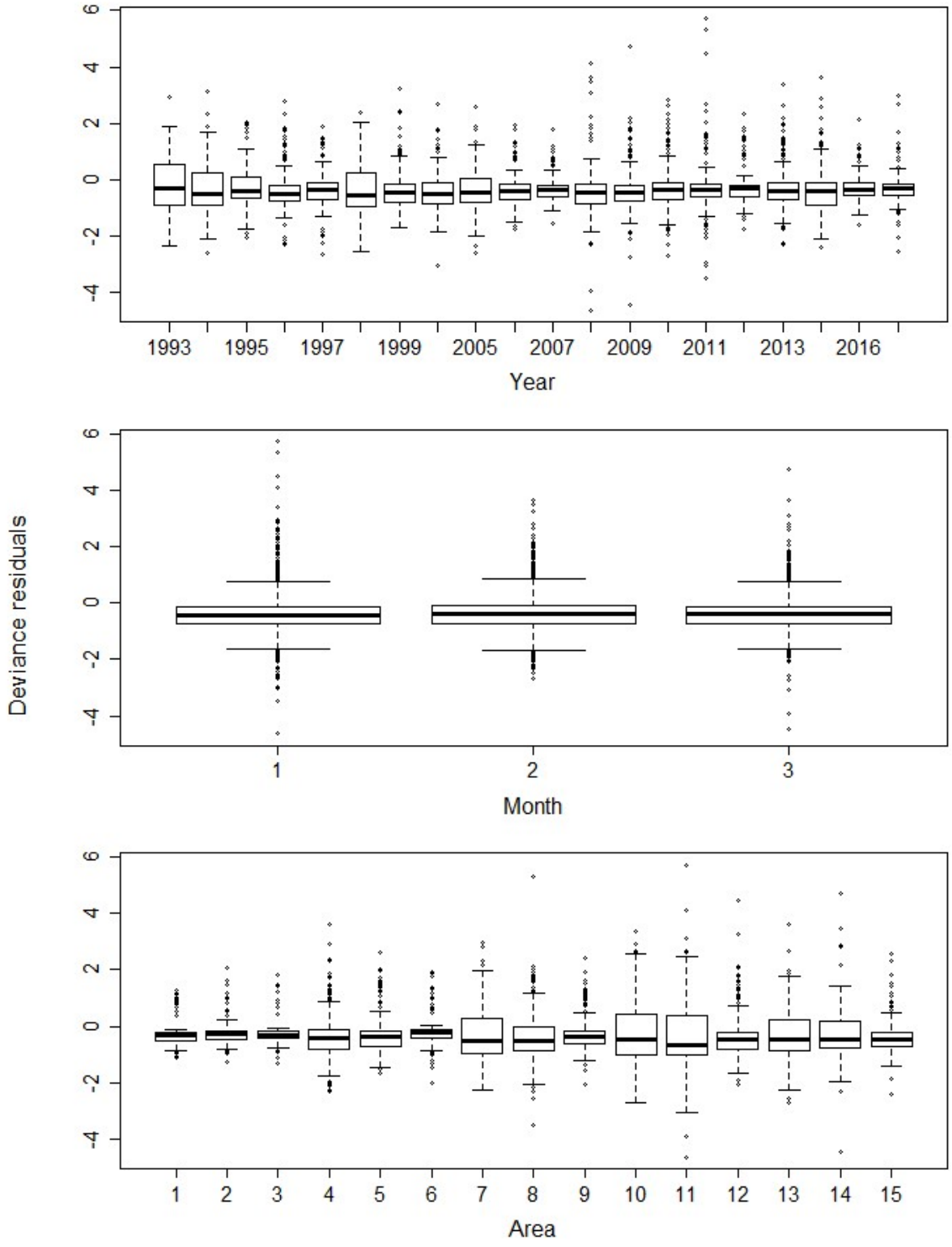

CONTACT US

t 1300 363 400
+61 3 9545 2176
e csiroenquiries@csiro.au
w www.csiro.au

AT CSIRO, WE DO THE EXTRAORDINARY EVERY DAY

We innovate for tomorrow and help improve today – for our customers, all Australians and the world.

Our innovations contribute billions of dollars to the Australian economy every year. As the largest patent holder in the nation, our vast wealth of intellectual property has led to more than 150 spin-off companies.

With more than 5,000 experts and a burning desire to get things done, we are Australia's catalyst for innovation.

CSIRO. WE IMAGINE. WE COLLABORATE. WE INNOVATE.

FOR FURTHER INFORMATION

Oceans & Atmosphere
Jessica Farley
t +61 6 6232 5189
e jessica.farley@csiro.au
w www.csiro.au

Oceans & Atmosphere
Paige Eveson
t +61 6 6232 5015
e paige.eveson@csiro.au
w www.csiro.au

Data61
Mark Bravington
t +61 6 6232 5118
e mark.bravington@data61.csiro.au
w www.data61.csiro.au